Journal of Electrical and Computer Engineering Innovations
(JECEI)
Journal homepage: http://www.jecei.sru.ac.ir

Research paper

Segmentation of Skin Lesions in Dermoscopic Images Using a Combination of Wavelet Transform and Modified U-Net Architecture

S. Fooladi, H. Farsi, S. Mohamadzadeh *

Department of Electrical Engineering, Faculty of Electrical and Computer Engineering, University of Birjand, Birjand, Iran.

Article Info

Article History:
Received 27 July 2024
Reviewed 12 September 2024
Revised 15 October 2024
Accepted 23 October 2024

Keywords:
U-Net
Segmentation
skin lesion
Deep neural networks
wavelet transform
Feature fusion
Medical image

*Corresponding Author's Email Address:
s.mohamadzadeh@birjand.ac.ir

Abstract

Background and Objectives: The increasing prevalence of skin cancer highlights the urgency for early intervention, emphasizing the need for advanced diagnostic tools. Computer-assisted diagnosis (CAD) offers a promising avenue to streamline skin cancer screening and alleviate associated costs.
Methods: This study endeavors to develop an automatic segmentation system employing deep neural networks, seamlessly integrating data manipulation into the learning process. Utilizing an encoder-decoder architecture rooted in U-Net and augmented by wavelet transform, our methodology facilitates the generation of high-resolution feature maps, thus bolstering the precision of the deep learning model.
Results: Performance evaluation metrics including sensitivity, accuracy, dice coefficient, and Jaccard similarity confirm the superior efficacy of our model compared to conventional methodologies. The results showed a accuracy of %96.89 for skin lesions in PH2 Database and %95.8 accuracy for ISIC 2017 database findings, which offers promising results compared to the results of other studies. Additionally, this research shows significant improvements in three metrics: sensitivity, Dice, and Jaccard. For the PH database, the values are 96, 96.40, and 95.40, respectively. For the ISIC database, the values are 92.85, 96.32, and 95.24, respectively.
Conclusion: In image processing and analysis, numerous solutions have emerged to aid dermatologists in their diagnostic endeavors The proposed algorithm was evaluated using two PH datasets, and the results were compared to recent studies. Impressively, the proposed algorithm demonstrated superior performance in terms of accuracy, sensitivity, Dice coefficient, and Jaccard Similarity scores when evaluated on the same database images compared to other methods.

Introduction

Over recent decades, there has been a notable rise in the incidence of skin cancer, underscoring the escalating significance of its initial treatment. Melanoma, the most lethal form of skin cancer, ranks among the most aggressive malignancies [1]. Automated segmentation of skin lesions in dermoscopic images is a crucial initial stage in utilizing computer assistance for diagnosing melanoma. Nonetheless, accurately discerning between benign and malignant skin lesions can be challenging, as there are considerable differences in lesion appearance across various patients. This ambiguity poses a diagnostic challenge even for seasoned medical professionals. Recent advancements in medical image processing have provided more effective techniques to aid dermatologists in diagnosing and classifying skin lesions. Therefore, computer-aided diagnosis (CAD) has become an indispensable tool for physicians and dermatologists,

especially when dealing with many patients in a short period [2]. The onset of this disease initiates with the impairment of skin cells, often instigated by ultraviolet radiation, resulting in mutations that prompt the rapid multiplication of skin cells, culminating in the development of cancerous growths. While typically characterized by a regulated and systematic growth pattern, specific newly generated cells may undergo unregulated proliferation, resulting in the formation of a cluster of malignant cells [3]. Early indications of melanoma often include alterations in the shape, size, and color of an individual's mole. Typically, melanomas exhibit a border that is black or blue-black in hue [3].

Automated skin lesion analysis relies heavily on segmentation, a crucial yet challenging process. Broadly, there are three main types of skin cancer:

(a) Basal Cell Carcinoma (BCC),

(b) Squamous Cell Carcinoma (SCC), and

(c) Melanoma (MM).

Segmentation essentially involves dividing an image into significant regions, with semantic segmentation specifically attributing suitable class labels to each region. In skin lesions, this typically entails two primary operations to delineate the lesion from the surrounding skin. The diagnosis of skin cancer is complex due to the diverse appearance of various skin lesions, notably Melanoma and Nevi, which pose challenges in differentiation. Despite the utilization of dermoscopy, a non-invasive diagnostic method, dermatologists' accuracy in diagnosing melanoma ranges from 75% to 84%. However, a biopsy offers a more precise diagnosis, albeit invasive and unpleasant for the patient. To prevent unnecessary biopsies, researchers have investigated various non-invasive methods for diagnosing melanoma [4]. These methods typically involve two stages: 1. Feature extraction, 2. Boundary (extent) identification of the skin lesion. Lesion segmentation is also useful as a preprocessing step when analyzing images with broad fields and multiple lesions. Effective clinical management of skin lesions relies heavily on timely diagnosis and accurate delineation of lesion boundaries to precisely identify the cancerous area for localization. Dermoscopy, employing visible light magnification, offers a more intricate skin examination compared to naked eye observation. We introduce a fully automated framework for precise detection and segmentation of lesion boundaries. This is accomplished by integrating a deep learning model with a wavelet transform map derived from specific kernel filters. The structure of this article is as follows:

Section 2 reviews existing literature in the field, highlighting significant contributions and advancements. Section 3 outlines the methodology proposed in this study, detailing the approach adopted for skin lesion segmentation. Section 4 presents the findings and results obtained through experimentation and evaluation of the proposed method. Finally, in Section 5, a comprehensive conclusion is drawn, summarizing the key insights gained from the research and outlining future directions for further investigation.

In recent years, significant advancements have been made in the field of medical imaging through various image processing techniques. One of the main challenges in this field is the precise and automatic segmentation of medical images for disease diagnosis and analysis. Medical image segmentation plays a crucial role in the early diagnosis and effective treatment of diseases. However, the accuracy and efficiency of existing algorithms still require improvement [2].

Deep neural networks, particularly the U-Net architecture, have been recognized as one of the successful architectures for medical image segmentation. U-Net, with its specific architectural design, is capable of extracting detailed and precise features from medical images. Nonetheless, it still faces limitations such as the need for a large volume of training data and high computational resource consumption [2].

One potential solution to improve U-Net's performance is the use of image preprocessing techniques such as wavelet transform. Wavelet transform, with its multi-resolution analysis capability, allows for the extraction of important and subtle features in medical images. These features can enhance segmentation accuracy and improve the performance of neural networks.

Therefore, the aim of this research is to investigate and propose a hybrid method combining wavelet transform and U-Net for improving medical image segmentation. It is expected that this approach will lead to increased accuracy and reduced segmentation errors in medical images, ultimately aiding in the timely diagnosis and treatment of diseases.

Using deep learning, it is possible to segment and detect various tumor tissues in medical images. Despite the potential difficulties, the accuracy of identifying and segmenting lesions in medical images is often accompanied by errors. An accurate and automated alternative to subjective and manual segmentation is segmentation using deep learning and computer systems. This method can achieve higher accuracy and be performed in a shorter time.

Given the deep network methods used for medical image segmentation, this research aims to leverage the strengths of various methods in the proposed model, ultimately leading to:

- Improved segmentation quality
- Reduced number of network parameters
- Reduced loss function

Related Work

In recent years, there has been notable interest among researchers in the pattern recognition and medical image processing domains towards automatic Computer-Aided Diagnosis (CAD) systems. The interest in image-based computer-aided diagnosis (CAD) systems has surged due to advancements in artificial intelligence and machine learning techniques. These developments have paved the way for creating CAD systems that utilize machine learning methods to analyze images, particularly for screening and early detection of malignant melanoma. As a result of recent technological and practical advancements, several emerging research and development areas have emerged. These areas have witnessed significant contributions from numerous researchers, resulting in a diverse range of CAD approaches and techniques. These advancements aim to assist dermatologists in automatically diagnosing melanoma from both dermoscopic and non-dermoscopic images [5], [6]. Lesion segmentation is an essential step for automatic melanoma detection. Numerous algorithms have been proposed by different researchers using various datasets employing methods such as thresholding, active contour, supervised and unsupervised techniques for segmenting dermoscopic skin lesion images. Automatic segmentation faces many challenges such as multicolor lesions, darkness at lesion boundaries, low contrast between lesion and normal skin, artifacts such as hair in the lesion area, and air bubbles due to gel applied to the skin in dermoscopy. The most commonly used methods for segmentation of skin lesions are traditional methods such as threshold based methods, clustering methods and correlated methods [7], [8]. Generally, threshold-based methods are used to extract regions of interest based on pixel intensity values. Therefore, image thresholding in grayscale transforms the image into a binary image separating the foreground from the background. Recently, research results have shown that deep learning models significantly contribute to medical image analysis for segmentation and Segmentation purposes [9], [10]. In their study [11], researchers introduced a hierarchical framework for skin lesion segmentation. Their approach involved an initial non-coherent operation, followed by passing the data to MASK RCNN for lesion segmentation. In the subsequent stage, they adapted a pre-trained DenseNet201 model and extracted features from two layers. These extracted features underwent refinement and enhancement using a combined selection block and were optimized using the salient optimization algorithm. The experimental evaluation was conducted on three dermoscopic datasets, demonstrating the enhanced performance of their proposed method. In their work [12], an intelligent framework for multi-class skin lesion segmentation was introduced. The method involved the initial segmentation of skin lesions using MASK RCNN. During this segmentation process, a 24-layer CNN model was employed, utilizing three datasets for the segmentation phase alongside the HAM10000 dataset. In their study [13], a Computer-Aided Diagnosis (CAD) system for localizing skin lesions was introduced. The process began with an initial incoherent operation by passing the data to MASK RCNN for lesion segmentation. Subsequently, they adjusted a pre-trained DenseNet201 model, extracting features from two layers. These features underwent refinement and enhancement using a combined selection block. The experimental evaluation was conducted on dermoscopic datasets, showcasing improved performance. In their paper [14], they presented a deep learning architecture tailored for skin lesion segmentation. The approach began by selecting the most optimal features to enhance the representation of lesion areas. Subsequently, an initial RCNN was deployed for the final segmentation of lesions. Dermoscopic datasets were utilized for evaluation purposes, demonstrating an enhancement in accuracy. In [15], an alternative segmentation method named "Fast Learning Artificial Neural Network" (FLANN) was introduced, serving as the foundation for an image segmentation technique. The study initiated noise reduction in the initial phase, employing a mean filter (3×3) to mitigate color distribution disparities. Following this step, pixels or neurons were converted into the R-G-B-S-V space via HSV conversion. FLANN clustering was then utilized to produce image clustering results, effectively segregating pixels of identical colors. Each image segment was allocated a distinct identifier, with close attention given to neighborhood size and tolerance effects.

In [16], a pioneering approach to skin lesion detection is presented, integrating uniform segmentation and feature selection into a cohesive strategy. This method encompasses various stages including preprocessing, lesion segmentation, feature extraction, feature selection, and final segmentation. Through a sequentially serial process, features such as color, texture, and HOG shape are extracted and combined. Subsequently, the Boltzmann entropy technique is employed for feature selection, followed by SVM classification. The effectiveness of this method is evaluated using the PH2 dataset, achieving promising results with a reported sensitivity of 97.7%, specificity of 96.7%, accuracy of 97.5%, and F-score of 97.5%.

In [17], a notable advancement in artificial hair removal was demonstrated through the fusion of deep learning and image processing techniques, yielding an accuracy of 85%. The study harnessed the Unet model for lesion segmentation, supplemented by image processing algorithms. Mainly, a Gaussian filter was applied to

diminish image noise. In contrast, [18] focused on enhancing accuracy by employing encoders like EffectNet and ResNet, achieving an accuracy of nearly 86% with the ResNet network. Furthermore, Shin et al. [19] introduced the DSM model, implementing strategies to refine segmentation accuracy by eliminating image noise and enhancing contrast.

In their study [20], researchers employed an extended U-Net network for medical image segmentation, capitalizing on the benefits of the U-Net architecture, including its compactness and skip connections. Additionally, they integrated bidirectional ConvLSTM and dense convolution mechanisms. The study focused on enhancing segmentation performance by incorporating Squeeze and Excitation modules, aiming to minimize complexity while improving results.

In their work [21], researchers introduce a multi-scale U-Net for skin lesion segmentation to address challenges like significant variations in texture and shape. This approach enhances hierarchical modeling by integrating an attention mechanism. Furthermore, it employs a bidirectional convolutional long short-term memory (BDCLSTM) structure to capture essential distinguishing features while suppressing less informative elements.

In [22], a novel segmentation method is proposed using fully convolutional networks (FCNs). This approach directly learns the full-resolution features of each pixel from the input data, eliminating the need for preprocessing or post processing operations such as artifact removal, low-contrast adjustment, or additional enhancements to improve the delineation of segmented skin lesions.

In [23], an enhanced skin lesion segmentation model based on U-Net++ is introduced to improve survival rates for melanoma patients and overcome associated challenges. A novel loss function is introduced to enhance the Jaccard segmentation index for skin lesion segmentation. Experimental results show the model's outstanding performance in segmenting the ISIC2018 I dataset, achieving an impressive Jaccard index of 84.73%. This method improves the Jaccard segmentation index for skin lesion images, aiding dermatologists in identifying and diagnosing various skin lesions while accurately delineating boundaries between lesions and normal skin.

In [18], the study presents an automated approach for segmenting lesion boundaries by combining two architectures, U-Net and ResNet, into a unified framework called Res-Unet. Moreover, image colorization eliminates unwanted hair, leading to notable enhancements in segmentation outcomes.

In [24], an exceptionally effective segmentation method is proposed to address challenges like unwanted residues (hair), uncertain boundaries, variable contrast, shape differences, and color variations in skin lesion images. The method introduces an improved FCN architecture (iFCN) tailored for segmenting high-resolution skin lesion images without needing preprocessing or post-processing. Leveraging residual structures within the FCN architecture, along with spatial information, enhances segmentation accuracy significantly.

In the study described in [25], a new CNN architecture is introduced, utilizing auxiliary information to enhance segmentation performance. Edge prediction is incorporated as an auxiliary task, running simultaneously with the main segmentation task. A cross-connection layer module is introduced, allowing intermediate feature maps from each task to influence the sub-blocks of other tasks. This approach implicitly guides the neural network to focus on the boundary area crucial for accurate segmentation.

In the study outlined in [26], two innovative end-to-end segmentation models, FBUNet-1 and FBUNet-2, are introduced. FBUNet-1 surpasses the performance of the traditional U-Net architecture by addressing spatial information loss during convolution operations. Building upon the progress of FBUNet-1, FBUNet-2 further improves accuracy by refining the loss function based on FBUNet-1's insights.

- U-Net Based Segmentation Techniques

In some articles: Introduced the U-Net architecture, which became a seminal work in the field of medical image segmentation. The U-Net's encoder-decoder structure, coupled with skip connections, enables precise localization and contextual understanding, making it effective for segmenting medical images such as MRI and CT scans. However, the model requires a large amount of annotated data and significant computational resources.

In some articles: Extended the U-Net architecture to 3D U-Net for volumetric medical image segmentation. This extension maintained the benefits of the original U-Net but adapted it to 3D data, which is essential for applications involving volumetric data such as MRI. The challenge remained in the increased computational cost and memory usage.

In some articles: Proposed a hybrid approach combining U-Net with conditional random fields (CRFs) to refine the segmentation output. The CRFs helped in capturing fine details and addressing segmentation boundaries more effectively. While the method improved accuracy, it also introduced additional complexity and computational overhead.

- Wavelet Transform in Medical Imaging

In some articles: Applied wavelet transform for ECG signal processing, showcasing its versatility beyond imaging. The study highlighted the wavelet's capability in dealing with non-stationary signals, an attribute valuable

in dynamic medical imaging contexts.

- Hybrid Approaches Combining U-Net and Other Techniques

In some articles: Introduced Attention U-Net, which incorporated attention mechanisms into the U-Net architecture to focus on relevant parts of the image. This approach aimed to enhance the model's ability to distinguish between foreground and background, improving segmentation accuracy without significantly increasing computational demands.

In some articles: Proposed UNet++ with nested and dense skip connections to address the issues of semantic gap between encoder and decoder. The model achieved better segmentation results but at the cost of increased complexity and training time.

In some articles: Combined U-Net with dilated convolutions to capture multi-scale context without reducing the resolution. This method aimed to improve the receptive field of the network, enhancing its ability to segment larger structures in medical images.

- Deep Learning for Medical Image Segmentation Beyond U-Net

In some articles: Provided a comprehensive survey of deep learning techniques for medical image analysis, including segmentation, classification, and detection. The review highlighted the dominance of CNN-based architectures and the emerging trends in integrating other techniques like GANs for improving segmentation.

In some articles: Reviewed various deep learning models for medical image segmentation, focusing on the strengths and weaknesses of different approaches. The study emphasized the importance of model robustness and generalizability across different datasets and imaging modalities.

In some articles: Discussed the use of transfer learning and multi-task learning in medical image segmentation, stressing the need for models that can leverage pre-trained knowledge and simultaneously learn related tasks for improved performance.

The reviewed literature highlights several key trends and insights in the field of medical image segmentation:

- U-Net and Its Variants: The U-Net architecture and its extensions (3D U-Net, Attention U-Net, UNet++) have proven highly effective for medical image segmentation. These models leverage skip connections and multi-scale feature extraction to achieve high accuracy. However, they require large datasets and significant computational resources, which can be a limitation in practical applications.

- Wavelet Transform: Wavelet transform offers a robust method for feature extraction and enhancement in medical imaging. Its multi-resolution analysis capability complements deep learning models by providing detailed spatial and frequency information, which is crucial for accurate segmentation.

- Hybrid Approaches: Combining U-Net with other techniques such as attention mechanisms, CRFs, and dilated convolutions can further enhance segmentation accuracy. These hybrid models address specific limitations of the original U-Net by improving feature localization, boundary detection, and multi-scale context understanding.

- Beyond U-Net: While U-Net remains a dominant architecture, other deep learning models and techniques are also being explored. The integration of transfer learning, multi-task learning, and GANs shows promise in enhancing segmentation performance and addressing challenges like data scarcity and model generalizability.

The literature suggests that while U-Net and its variants are highly effective for medical image segmentation, there is still room for improvement in terms of accuracy, computational efficiency, and robustness. Hybrid approaches that integrate wavelet transform and other techniques offer a promising direction for future research. Additionally, exploring alternative deep learning models and leveraging advanced techniques like transfer learning and multi-task learning could further advance the field and lead to more practical and reliable segmentation solutions.

Regarding the limitations of previous works, it can be noted that traditional methods were often used for feature extraction. In our research, however, we utilize deep learning-based methods for this purpose.

By leveraging the strengths of the mentioned works in this research, the use of mutual connection modules is proposed. In these modules, the intermediate feature maps of each task are fed into the sub-blocks of other tasks, which can implicitly guide the neural network to focus on the boundary region of the segmentation task.

Proposed Method

Block Diagram 2 provides an overview of the skin lesion segmentation in skin images. The proposed method initiates by extracting the feature map of the images utilizing wavelet transform, followed by selecting top features using selected feature algorithms. Subsequently, a fully automated architecture is introduced for precise lesion boundary detection and segmentation. This architecture pairs a deep learning model with the feature map derived from specific kernel filters of wavelet transform. By integrating the feature maps of wavelet transform with a deep learning U-Net model trained end-to-end, our method effectively reduces the number of trainable parameters.

The Fourier transform is used to represent the frequency properties of a signal by decomposing the

signal into different sinusoids. However, this method does not provide simultaneous signal resolution in both the time and frequency domains and gives less information for signals with varying frequency over time.

We chose Wavelet Transform for our analysis due to its ability to effectively capture both time and frequency domain characteristics of signals, making it suitable for analyzing non-stationary signals. Unlike the fixed window length constraint of Short-Time Fourier Transform (STFT), Wavelet Transform offers more flexibility, allowing for better adaptation to varying signal properties.

Wavelet transform is a fundamental mathematical tool with diverse applications across scientific fields. It addresses the limitations of the Fourier transform by excelling in analyzing non-stationary signals and dynamic systems. Unlike the Fourier transform, wavelets exhibit localization properties in both space and frequency domains. This unique characteristic enables examining spatial frequency content in signals without sacrificing positional information. Therefore, wavelet transform offers a valuable balance between pixel and Fourier space representation. The wavelet transform harnesses various essential features, including spatial localization, frequency band tuning, directionality, scale and rotational similarities, and quadrature phase. It operates through a collection of mother wavelets and a scaling equation dictating the movements of these wavelets via scaling and translation. This transformation comprises eight mother wavelets grouped into four pairs, each characterized by distinct orientations (0°, 45°, 90°, and 135°). Each pair consists of one odd-symmetric and one even-symmetric wavelet, symbolized by ϕ and ψ. The eight mother wavelets are denoted as ψ_1,...,ψ_8. Let's define a two-dimensional pulse u(x, y) [26]:

$$u(x,y)\begin{cases}1 \text{ if } 0<x\le 1,\ 0<y\le 1\\ 0 \text{ otherwise}\end{cases} \tag{1}$$

Next, we identify the four pairs of mother wavelets as follows [26]:

$$\beta_{0,e}(x,y)=\left[-u\left(x,y/3\right)+2u(x-1,y/3)-u\left(x-2,y/3\right)\right]/\sqrt{18} \tag{2}$$

$$\beta_{0,O}(x,y)=\left[-u\left(x,y/3\right)+u(x-2,y/3)\right]/\sqrt{6} \tag{3}$$

$$\beta_{45,e}\left(x,y\right)=\begin{bmatrix}-\left(u\left(x,(y-1)/2\right)+u\left(x-1,y\right)+u\left(x-1,y-2\right)+u\left(x-2,y/2\right)\right)\\ +2(u\left(x,y\right)+u\left(x-1,y-1\right)+u\left(x-2,y-2\right))\end{bmatrix}/\sqrt{18} \tag{4}$$

$$\beta_{45,o}(x,y)=\begin{bmatrix}-u(\left(x,y-2\right)+u(x-1,y)+u\left(x-2,y-1\right))+u(x,y-1)\\ +u\left(x-1,y-2\right)+u\left(x-2,y\right)\end{bmatrix}/\sqrt{6} \tag{5}$$

$$\beta_{90,o}\left(x,y\right)=\left[u\left(x/3,y\right)-u\left(x/3,y-2\right)\right]/\sqrt{6} \tag{6}$$

$$\beta_{90,e}\left(x,y\right)=\left[-u\left(x/3,y\right)+2u\left(x/3,y-1\right)-u\left(x/3,y-2\right)\right]/\sqrt{18} \tag{7}$$

$$\beta_{135,o}\left(x,y\right)=\begin{bmatrix}-(u\left(x,y\right)+u\left(x-2,y-1\right)+u\left(x-1,y-2\right))\\ +u\left(x,y-1\right)+u\left(x-1,y\right)+u\left(x-2,y-2\right)\end{bmatrix}/\sqrt{6} \tag{8}$$

$$\beta_{135,e}\left(x,y\right)=\begin{bmatrix}-(u\left(x,y/2\right)+u\left(x-1,y\right)+u\left(x-1,y-2\right))\\ +u\left(x-2,(y-1)/2\right)+2u((x,y-2)+u\left(x-,y-1\right)\\ +u\left(x-2,y\right))\end{bmatrix}/\sqrt{18} \tag{9}$$

Mother wavelets are piecewise constant functions, so that each wavelet $b_{\varphi,\phi}$ can be fully described by a 3×3 matrix.

Fig. 1 illustrates eight mother wavelets, demonstrating the transformation process. Part A showcases these wavelets in pixel space, while Part B exhibits the discrete Fourier transform (DFT) of the 3×3 mother wavelets. The selection of wavelets is such that each DFT encompasses a pair of pixels, minimizing their spatial frequency and bandwidth orientation within this space.

Furthermore, to ensure orthogonality, four pairs of wavelets are included, each oriented in one of four different directions (0°, 45°, 90°, and 135°). These pairs are composed of one wavelet with a real symmetric even DFT, corresponding to an even symmetric function in pixel space, and the other wavelet with an imaginary symmetrical odd DFT, corresponding to an odd symmetrical function in pixel space. The 3×3 DFTs allow qualitative similarity to Gabor filters. The 3×3 DFTs bear qualitative resemblance to Gabor filters. As the wavelets undergo higher-resolution decomposition, they occupy less space in the Fourier domain [26].

$b_{0,e}=\frac{1}{\sqrt{18}}\begin{bmatrix}-1&2&-1\\-1&0&-1\\-1&0&-1\end{bmatrix}$	$b_{0,o}=\frac{1}{\sqrt{6}}\begin{bmatrix}-1&-1&-1\\0&0&0\\1&1&1\end{bmatrix}$
$b_{90,o}=\frac{1}{\sqrt{6}}\begin{bmatrix}-1&-1&-1\\0&0&0\\1&1&1\end{bmatrix}$	$b_{45,o}=\frac{1}{\sqrt{18}}\begin{bmatrix}-1&1&0\\1&0&-1\\0&-1&1\end{bmatrix}$
$b_{90,e}=\frac{1}{\sqrt{18}}\begin{bmatrix}-1&-1&-1\\2&2&2\\-1&-1&-1\end{bmatrix}$	$b_{90,o}=\frac{1}{\sqrt{6}}\begin{bmatrix}-1&-1&-1\\0&0&0\\1&1&1\end{bmatrix}$
$b_{135,e}=\frac{1}{\sqrt{18}}\begin{bmatrix}2&-1&-1\\-1&2&-1\\-1&-1&2\end{bmatrix}$	$b_{135,o}=\frac{1}{\sqrt{6}}\begin{bmatrix}0&-1&1\\1&0&-1\\-1&1&0\end{bmatrix}$

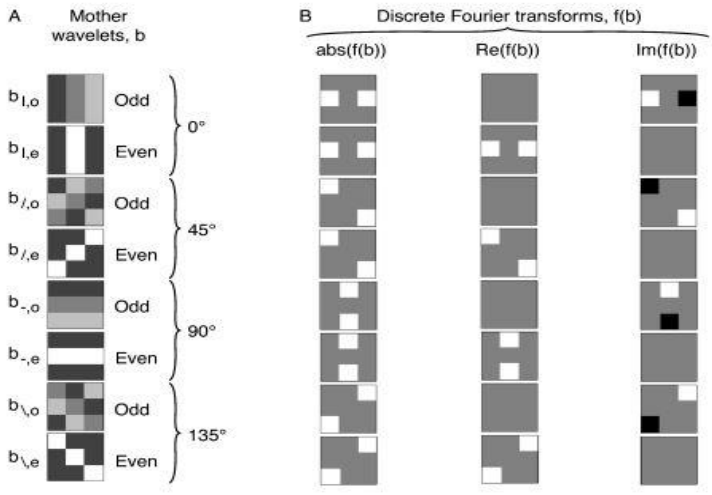

Fig. 1: Eight mother wavelets.

Feature selection involves identifying pertinent features while discarding irrelevant and redundant ones, intending to obtain a subset of features that adequately describes the problem with minimal loss of performance. Essentially, it is the process of selecting the most essential features to represent the data accurately. This task significantly improves the proposed method by removing irrelevant features and presenting the most useful ones. Some advantages of feature selection in our research include:

- Enhancing the performance of machine learning algorithms.
- Facilitating understanding of data and gaining insights into the underlying processes, aiding visualization.
- Decreasing overall data volume, thereby reducing storage requirements and potentially cutting costs.
- Streamlining the feature set, which can save resources in future data collection or utilization phases.
- Promoting simplicity and enabling simpler models, thereby enhancing speed and efficiency.

To identify a relevant feature for the problem, the study employs the following definition: a feature is deemed relevant if it holds information pertinent to the objective.

In this research, significant factors are considered to enhance the accuracy of the proposed method within the feature selection framework.

The initial stage of the proposed method involves identifying the nearest neighbors from a subset of samples randomly selected from the dataset. For each chosen sample, the feature values are compared to those of its nearest neighbors, and the scores of each feature are adjusted accordingly.

This methodology is rooted in assessing feature quality by gauging the degree of variation in their values among neighboring samples.

In the second stage of the feature selection method, correlation-based feature selection (CFS) is employed. This method deems a subset of features as favorable if, on the one hand, they exhibit a strong correlation with the target feature and, on the other hand, they are minimally correlated with each other. In this research, the merit or goodness of a feature subset is computed using the following formula [2]:

$$Merit_{s_k} = \frac{k\bar{r}_{cf}}{\sqrt{k + k(k-1)\bar{r}_{ff}}} \tag{10}$$

In this formula, $\bar{r}_{cf}$ the first term represents the average correlation between the target feature and $\bar{r}_{ff}$ all the features present in the dataset, while the second term represents the average pairwise correlation calculated among the features. Ultimately, the correlation-based method is formulated as follows [2]:

$$CFS = \max_{s_k}\left[\frac{r_{cf1}+r_{cf2}+\ldots\ldots+r_{cfk}}{\sqrt{k+2\left(r_{f2f1}+\ldots.+r_{fifj}+\ldots.+r_{fkf1}\right)}}\right] \tag{11}$$

In this equation, the variables r_{cfi} , r_{fifj} represent the correlation values. The correlation-based method is used for selecting the best features.

Next, the Recursive Feature Elimination (RFE) method is introduced, employing a multivariate mapping approach that iteratively constructs a model and selects the most discriminative features, whether the best or worst-performing ones.

In RFE, all voxels within a region, constituting the smallest unit of a three-dimensional image structure, are considered. Voxels that do not contribute to distinguishing features among different classes are progressively eliminated. Features are then ranked according to the order of their elimination. Thus, this method operates as a greedy optimization technique to identify the optimal subset of features.

Lastly, all features undergo decoding via statistical hypothesis testing, and each feature is ranked based on its values. Feature weights are determined utilizing the chi-square statistical method. A function evaluates the significance of a feature by computing the chi-square statistic and subsequently ranks the features accordingly, taking into account their respective classes. This ranking procedure is executed to compare the features and identify their relative importance.

Features selected through the above methods often have different ranges, and classifiers typically require normalized features because their values fall within a specific range. One of the most common normalization methods is the z-score normalization method [2]:

$$Z = (x - \mu)/\sigma \tag{12}$$

where μ denotes the mean and σ denotes the standard deviation from the mean. This method generates a range of values between 0 and 1. Below is Algorithm 1 outlining the overall process of this research in the form of pseudocode.

As can be seen in Fig. 2, the proposed method uses a number of unique methods to extract features and normalizes the features that often have different ranges to a specific range by using the score method.

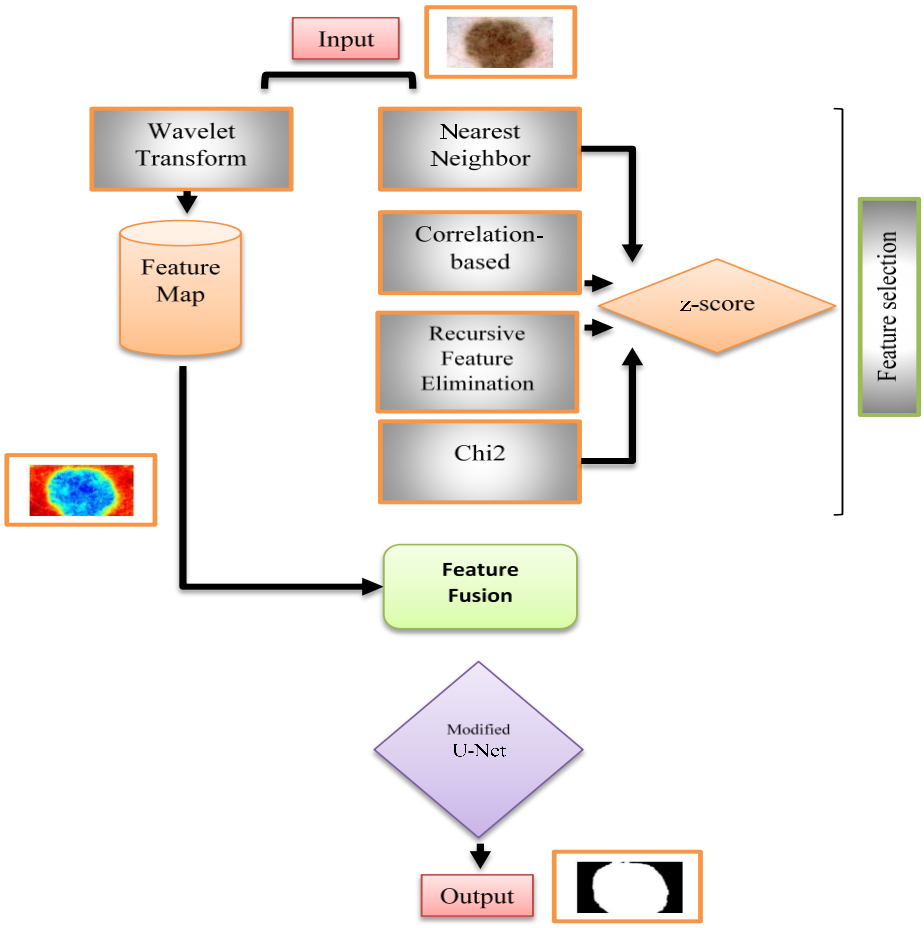

Fig. 2: Sequence of components in the proposed method.

Algorithm 1: Algorithm of the proposed method

Input:
trainImgSet: The medical images Set, with segmented skin lesion areas manually in theirs;
targets = The segmented skin lesion areas manually in *1*.trainImgSet.
get N = The number of images in trainImgSet
get wavelet = The wavelet transform according to Equation (1,2,..,9)
get NN = The Nearest Neighbor algorithm
get Cb= Correlation-based algorithm
get RFE= Recursive Feature Elimination algorithm
get ch = The Chi2 algorithm
get z_s = The z-score according to Equation (12)
get FM = The Feature Map resulting from wavelet transform
2.for i = 1 to N do:
WT[i]= wavelet(trainImgSet[i])
WT_b[i]= The Feature Map resulting from wavelet transform
Z [i] = The z-score features extracted of (NN,Cb, RFE, ch)
3.for region in the RI do :
RCI=U-Net(region)
add RCI to U-Net _Features
Selcted_features= Applying feature selection algorithm and Feature Map resulting from wavelet transform
4. Segmented_features=U-Net(Selcted_features)
Output:
Segmented_features = an image, that lesion pixels are distinguished.

Proposed Network Architecture

Fig. 3 illustrates the proposed architecture for the automatic segmentation of skin lesions. This method integrates wavelet transform feature maps and selected features via feature selection methods into a U-Net deep learning model trained end-to-end. The architecture comprises two encoder branches for abstract feature extraction and one decoder path for reconstruction.

The contraction path involves a sequence of convolutional and max-pooling layers aimed at reducing the size of the input image and extracting relevant features. Conversely, the expansion path comprises a sequence of convolutional and upsampling layers responsible for increasing the size of the feature maps obtained from the contraction path and integrating them with features from the input image to generate the final segmentation map. Skip connections allow information to bypass one or more levels within the expansion path and connect them to corresponding layers in the contraction path. These connections facilitate the transmission of high-level and low-level information from the input image to the model, thereby improving the accuracy of the final segmentation.

Broadly, the proposed architecture extracts features from the input image through the contraction path. These

features are then amalgamated with input image features via the expansion path and skip connections. Finally, the convolutional layers within the expansion path are employed to produce the final segmentation map.

The encoder architecture proposed in our study comprises seven convolutional layers and three max-pooling operations, each utilizing a stride of 2. These convolutional layers extract feature maps from the input image through 3x3 kernel convolutional operations. The study adopts a cautious approach to kernel sizes, starting with smaller kernels and gradually increasing them if necessary to avoid computational overhead and overfitting risks. To cover larger receptive fields without increasing the parameters linked to each kernel, expanded convolutional layers are utilized at every encoder level.

In addition, in order to reduce the size of the extracted feature maps, max-pooling operations are used. This process optimizes memory utilization by retaining only the pixel with the maximum value among the four neighboring pixels. However, it results in a loss of feature map resolution.

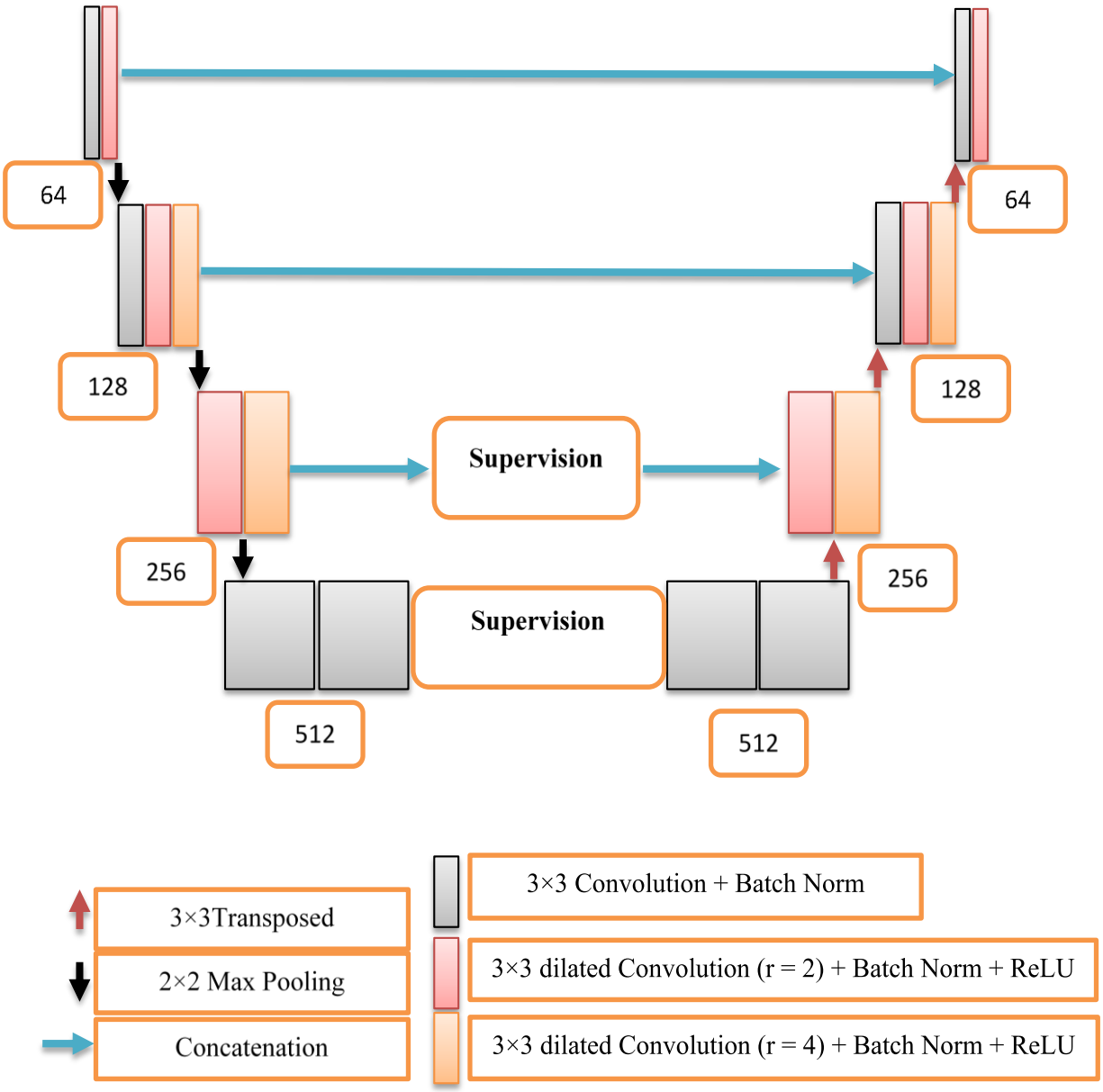

Fig. 2: Proposed architecture.

The encoder includes a convolutional block, consisting of two standardized convolutional layers in addition to the supervision layer and two other standard convolutional layers. The supervision block plays a crucial role in gathering information at various levels to incorporate more features. Meanwhile, the decoder utilizes alternating 3x3 deconvolutions to decrease the number of feature maps. Skip connections recover spatial information lost during pooling operations, following a similar approach to U-Net. Initially, the feature map is inputted to the control block and, except for the last stage, it will merge with corresponding maps from the decoder path. To generate the output segmentation map, the decoder employs a 1x1 convolution layer followed by a sigmoid layer, serving as a pixel-wise classifier. Each 3x3 convolution is accompanied by a batch normalization (BN) layer and a modified ReLU activation function to expedite the training process.

In the expanded convolution segment, drawing inspiration from reference [28], rather than downsampling feature maps at a low rate, the feature maps from the expanded convolution are harnessed for image segmentation. The receptive field of a kernel, denoted as k with a size of N×N, can be defined as follows [2]:

$$R_k = N + (N-1)(r-1) \tag{13}$$

In this equation, N = 3 (the kernel sizes are considered constant). The r represents the dilation rate, which specifies the spacing between values of the filter. In typical scenarios, r = 1 is assumed.

In this research, the supervision block is instrumental in refining localization and attaining more precise segmentation by directing attention to specific regions within an image. Within the proposed U-Net architecture, these supervision blocks aid in transferring essential features through skip connections. By leveraging contextual information, these blocks achieve a focus on specific regions. Before the concatenation operation, they effectively filter out noise and other irrelevant details from high-level features, ensuring accurate feature transmission.

Utilizing features extracted from deep networks leads to the identification of complex relationships in the image, thereby resulting in more precise segmentation results [34], [35].

The graphic view shown in Fig. 3 simply and in detail shows the proposed Unet network and its components.

Features extracted from deep networks help identify complex relationships within images, which directly lead to improved segmentation accuracy. Unlike traditional methods that may focus only on simple and distinct patterns in the data, deep networks, especially architectures like U-Net, are capable of learning features that not only capture high-level information (such as large structures) but also take into account fine details.

For example, in some studies, the use of deep networks for liver segmentation from CT scan images has demonstrated how these architectures can extract complex and precise features, providing significantly more accurate results compared to traditional methods. This improvement in accuracy is due to the ability of deep networks to learn various features across different layers, leading to segmentation results that are not only visually superior but also encompass finer and more detailed structures.

Moreover, in another study focused on enhancing the feature space using the deep network SqueezeNet, it has been observed that deep networks can lead to improved segmentation in textural images. This is particularly important in images with textural and complex patterns, as deep networks are capable of learning and recognizing intricate patterns in the images, resulting in a significant improvement in the final outcomes.

Results Database

The PH2 database results from collaborative efforts between the University of Porto, Instituto Superior Técnico Lisbon, and the Dermatology Services of Pedro Hispano Hospital in Matosinhos, Portugal. This database comprises 200 dermoscopic images, carefully curated to include 80 common nevi, 80 atypical nevi, and 40 melanomas. The selection process prioritized image quality, clarity, and the presence of dermoscopic features. Each image underwent evaluation by a dermatologist, considering parameters such as manual segmentation of the skin lesion, clinical diagnosis, histopathology (if available), and dermoscopic criteria, including asymmetry, colors, pigment network, dots/globules, streaks, and regression areas.

The ISIC2017 database, another crucial aspect of this study, consists of 2600 images designated for skin lesion analysis. Among these, 2000 images serve as training samples, while the remaining 600 images are reserved for testing purposes. The data used in this research consists of images captured with regular photographic cameras, not a specialized medical imaging camera.

The ISIC database is a public and open source for skin images. This database contains dermatological images with high quality and quality control. These images are used as a public resource for training, research and development and testing of diagnostic artificial intelligence algorithms. This database can be used to improve clinical diagnostic skills and provide support in skin cancer diagnosis. Also, the development and testing of algorithms for skin cancer triage and diagnosis also utilizes this database.

By using the database images shown in Fig. 4 and Fig. 5, the steps of the proposed method in Fig. 2 are performed in order and finally an effective division of the database images is presented as the output of the proposed network.

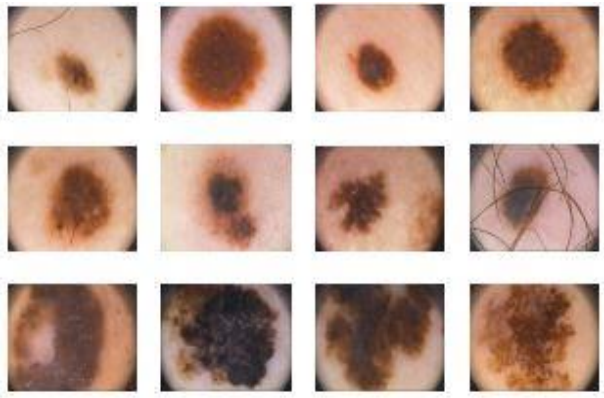

Fig. 4: A collection of images from the PH2 database, including common moles (first row), a typical moles (second row), and melanomas (third row).

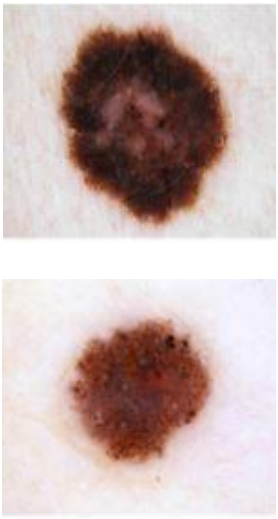

Fig. 5: A collection of images from the ISIC database.

Evaluation Criteria

In this section, the performance of the proposed method is validated by comparing the output information of deep learning with diagnostic data provided by specialized physicians in the community. The performance of the proposed skin lesion segmentation method is evaluated using various metrics including sensitivity, accuracy, dice coefficient, and Jaccard similarity.

TN (True Negatives) indicates the number of records that are actually negative, and the classification algorithm correctly identified them as negative.

TP (True Positives) represents the count of records that are truly positive, and the classification algorithm correctly classified them as positive.

FP (False Positives) represents the count of records that are actually negative, but the classification algorithm incorrectly classified them as positive.

FN (False Negatives) represents the count of records that are actually positive, but the classification algorithm incorrectly classified them as negative.

The ability to differentiate between diseased and healthy cases from other cases is referred to as accuracy. The mathematical expression of this concept is depicted in the following equation [31].

$$Accuracy = \frac{TN + TP}{TN + FN + TP + FP} \tag{14}$$

The accuracy metric does not distinguish between FN and FP. To overcome this issue, the precision metric is defined. The ability of a method to detect disease cases, lesion areas, and cancerous nuclei is called sensitivity. To calculate the sensitivity of a test, one must compute the ratio of true positive cases to the sum of true positive and false negative cases, as shown in the following mathematical expression [31].

$$sensitivity = \frac{TP}{TP + FP} \tag{15}$$

The maximum symmetric surface distance (MSSD), referred to as the Hausdorff distance, can be computed by calculating the maximum distance between the surface voxels of the predicted maps and the ground truth images, with 0 mm stands for perfect segmentation. where Ip and Iy are the predicted maps and ground truth, The shortest distance of a random voxel x to the set of surface voxels of Iy is stated as below Eq. [31].

$$d\left(x, I_y\right) = \min_{y \in I_y} \left\| x - y \right\| \tag{16}$$

It can be written as:

$$MSSD = \max \begin{pmatrix} \left(\max_{x \in I_p} d\left(x, I_d\right) \right) \\ , \left(\max_{y \in I_p} d\left(y, I_p\right) \right) \end{pmatrix} \tag{17}$$

Jaccard similarity is a frequently used metric for measuring the similarity between two objects, such as two images. It can be applied to assess the similarity between two asymmetric binary vectors or to gauge the similarity between two sets.

a. Represents the number of features equal to one for both objects i and j.

b. Indicates the number of features that are zero for object i but one for object j.

c. Denotes the number of features that are one for object i but zero for object j.

d. Refers to the number of features that are zero for both objects i and j.

$$J(i,j)=\frac{a}{a+b+c} \quad (18)$$

$$Jaccard=\frac{TP}{TP+FN+FP} \quad (19)$$

The Dice coefficient is widely employed to quantify the similarity between two images, although it can also be utilized for other data types. Essentially, it assesses the similarity and overlap between the ground truth and the predicted output.

The Dice coefficient serves as a fundamental metric for assessing the outcomes of medical image segmentation. This score quantifies the similarity between the segmentation results produced by a model and the true tissue mask.

$$dice=\frac{2TP}{2TP+FP+FN} \quad (20)$$

Output Results

In this section, the results of the proposed method are juxtaposed with those of other methods, illustrating enhancements in key parameters for image segmentation within the target database. The proposed U-Net architecture facilitates effective segmentation through the utilization of a limited number of training images, along with the integration of information obtained from both the encoder and decoder stages to generate an efficient segmentation map. Tables 1 and 2 present the outcomes of lesion segmentation using various methods, contingent upon the selecting features from the images. It is observed that the proposed method achieves superior segmentation accuracy and precision compared to alternative approaches. This superiority can be attributed to the feature extraction methodology employing deep learning networks and the amalgamation of different feature selections tailored to the structural characteristics of the database images.

Table 1: Results of skin lesion segmentation execution on the PH2 database

Methods	Accuracy	Sensitivity	Dice	Jaccard Similarity
MCGU-Net [20]	95.3	83.2	92.6	95.3
Multiscale Attention U-Net [21]	96.1	94.3	93.7	96.1
FrCN [22]	95.08	93.7	91.7	95.3
U-Net + + [23]	89.6	-	92.7	84.7
Res-Unet [18]	-	-	92.4	85.4
iFCN [24]	96.9	96.8	93.02	87.1
A novel CNN using auxiliary information [25]	94.32	88.76	-	79.46
Proposed method	**96.89**	**96**	**96.40**	**95.40**

Table 2: Results of skin lesion segmentation on the ISIC 2017 database

Methods	Accuracy	Sensitivity	Dice	Jaccard Similarity
deep residual networks [32]	93.40	80.20	84.40	76
fully convolutional-deconvolutional [33]	93.40	82.50	84.90	76.50
Proposed method	**95.98**	**92.85**	**96.32**	**95.24**

Fig. 6 illustrates the eight mother wavelets used in this study. The appropriate selection of the mother wavelet plays a key role in wavelet analysis. For example, in noise removal using wavelets, choosing the appropriate mother wavelet ensures that the most signal power is concentrated on a small number of wavelet coefficients, facilitating the separation of noisy and signal components through thresholding. Mother wavelets are categorized into different segments based on their properties. These properties include orthogonality, compact support, symmetry, and vanishing moments. The properties of mother wavelets are crucial in selecting a suitable mother wavelet. However, there often exist multiple mother wavelets with similar properties. In general, to address the challenge of selecting a mother wavelet, we need to consider the similarity between the signal and the mother

wavelet as a criterion.

The higher the similarity between the mother wavelet and a specific signal, the better signal decomposition into wavelet coefficients. There are various methods for determining the similarity between a signal and a mother wavelet based on qualitative and quantitative approaches. However, there is no single standard method for this selection.

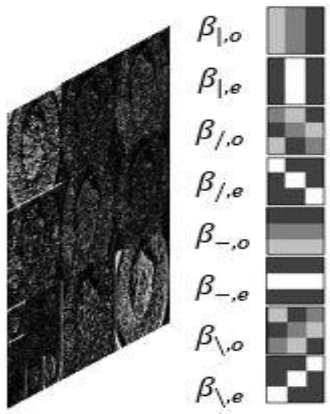

Fig. 6: a. Mother wavelets, b. Filter coefficients response to eight mother wavelets.

In the study [26], two convolutional neural network segmentation models, FBUNet-1 and FBUNet-2, based on the fusion block architecture for segmenting biomedical images, are introduced.

Tables 3 and 4 compare the results of the proposed method with these two methods, FBUNet-1 and FBUNet-2, which have been utilized for segmenting biomedical images of cells and blood vessels. The primary objective of these Tables is to showcase the superiority of the proposed method over the other two methods in handling various datasets comprising different biomedical images.

Table 3 and Table 4 not only demonstrate the superiority of the proposed method in three evaluation parameters, Sensitivity, Dice, and Jaccard Similarity, indicating the high efficiency of the proposed method in medical image segmentation, but also show a reduction in the number of parameters, leading to an increase in the speed of segmentation of the proposed method.

Table 3: Results of the proposed segmentation method compared with FBUNet-1 and FBUNet-2 for cell images

Method	Sensitivity	Dice	Jaccard Similarity	Parameters
FBUNet-1	93.66	93.58	88.41	5,097,925
FBUNet-2	94.19	93.84	88.62	5,098,356
Proposed method	**96**	**96.40**	**95.40**	**1,259,523**

Table 4: Results of the proposed segmentation method compared with FBUNet-1 and FBUNet-2 for blood vessel images

Method	Sensitivity	Dice	Jaccard Similarity	Parameters
FBUNet-1	74.23	79.03	65.16	5,097,452
FBUNet-2	75.64	79.15	65.53	5,098,001
Proposed method	**96**	**96.40**	**95.40**	**1,259,523**

In Table 5, it can be seen that the proposed module improves the basic level of U-Net in terms of MSSD criteria [34].

Table 5: The results of comparing the MSSD criteria

Method	MSSD
U-Net + baseline	50.039
U-Net + CBAM	29.524
U-Net +CoT	22.886
U-Net + ECA	38.402
Proposed method	17.641

Fig. 7 displays the feature maps obtained from the wavelet transform of the proposed method.

The feature map obtained is a visual representation of the frequency content of the image.

Feature maps in this research are used for pattern recognition, anomaly detection, or feature extraction from the signal.

Fig. 8 displays some of the segmentation results obtained by the proposed method. As observed from the visual results, our network generates smooth segmentation outputs in the border region, which is clinically very useful.

It is evident that our proposed method pays more attention to the border region, and this approach creates a smooth segmentation boundary without additional noisy areas.

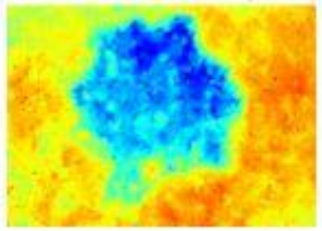

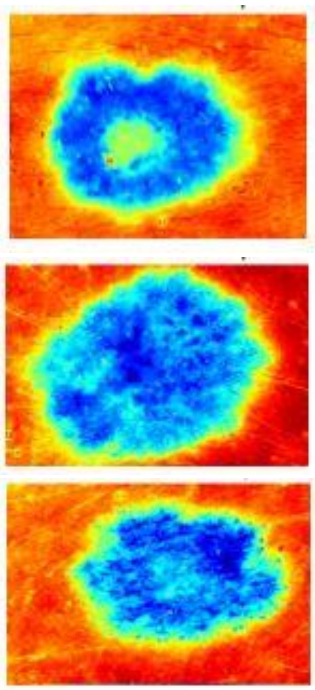

Fig. 7: Feature map obtained from wavelet transform.

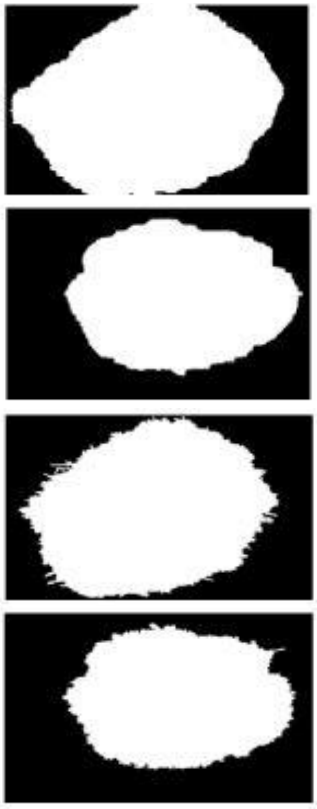

Fig. 8: First row. Ground truth second row. Predicted mask from the combination of wavelet transform and proposed architecture.

Fig. 9 outlines the boundary of the skin lesion by utilizing the output mask. Incorporating wavelet transform enhances the details of the skin lesion, thereby facilitating the development of a more refined algorithm for precise and automated segmentation of skin lesions.

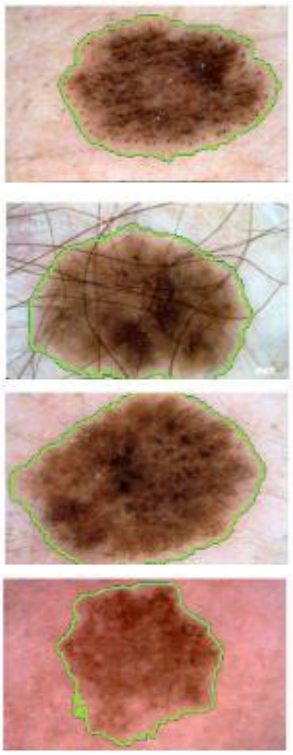

Fig. 9: Detected boundary of the skin lesion area.

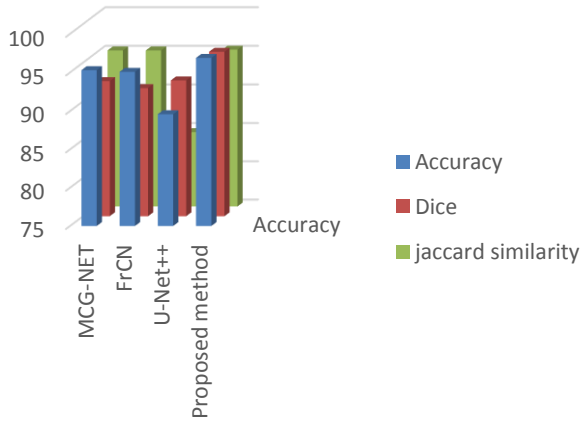

Fig. 10: Comparative plot of different methods for three evaluation metrics.

Fig. 10 illustrates a comparative plot of different methods across three important evaluation metrics in image segmentation. The detection speed in the proposed method is much higher than other methods proposed in previous research, which use low-level learning methods and human detection methods. This can be attributed to the hierarchical learning approach employed in the proposed method, leading to deep learning, feature vector reduction, and a decrease in the number of parameters.

Conclusion

In image processing and analysis, numerous solutions have emerged to aid dermatologists in their diagnostic endeavors.

This paper proposes a method for segmenting skin lesions in dermoscopic images, which tackles challenges like dense hair and gel by integrating wavelet transform and deep learning networks. Manual segmentation, a laborious task heavily reliant on operator expertise, underscores the need for fully automatic methods to delineate skin lesion extents precisely. Despite recent strides in automated algorithms for this purpose, challenges persist due to the diverse characteristics of skin lesions, including size, shape, spatial location, and appearance heterogeneity.

The proposed method significantly increases detection speed by using hierarchical learning and selecting important features, instead of low-level techniques. It improves U-Net performance with supervision blocks between encoding and decoding steps.

Suggestions for enhancing medical image segmentation with deep learning include:

- Improving Accuracy and Efficiency:

- Use multiscale neural networks and attention models.

- Enhancing Robustness:

- Implement data augmentation and transfer learning.

- Integrating Multimodal Information:

- Combine medical images with patient data and multiple models.

- Ensuring Explainability and Transparency:

- Develop methods to understand model decision-making.

- Reducing Computational Resources:

- Create lightweight and optimized models with compression techniques.

- Innovative Applications:

- Develop real-time segmentation models and detect rare diseases.

- Validation and Evaluation:

- Create standard datasets and conduct clinical studies.

These suggestions aim to develop effective and practical models for medical image segmentation, benefiting healthcare.

Author Contribution

S. Fooladi, H. Farsi, S. Mohamadzadeh designed experiments, S. Fooladi, H. Farsi and S. Mohamadzadeh have undertaken the design, execution and analysis of the study results. They also wrote the article and approved its final version.

Acknowledgment

We are grateful to all those who helped us in this research. This article has no financial resources.

Conflict of Interest

The authors state that they have no mutual interest in authoring or publishing the article.

Abbreviations

CAD	Computer-Assisted Diagnosis
BCC	Basal Cell Carcinoma
SCC	Squamous Cell Carcinoma
MM	Melanoma
CNN	Convolutional Neural Network
RFE	Recursive Feature Elimination

References

[1] A. Rehman, M. A. Butt, M. Zaman, "Attention Res-UNet: Attention residual UNet with focal Tversky loss for skin lesion segmentation," Int. J. Decis. Support Syst. Technol., 15(1): 1-17, 2023.

[2] M. K. Hasan, M. A. Ahamad, C. H. Yap, G. Yang, "A survey, review, and future trends of skin lesion segmentation and classification," Comput. Bio. Med., 106624, 2023.

[3] I. Ul Haq, J. Amin, M. Sharif, M. Almas Anjum, "Skin lesion detection using recent machine learning approaches," in Prognostic Models in Healthcare: AI and Statistical Approaches, pp. 193-211, Springer, 2022.

[4] S. Khattar, R. Kaur, "Computer assisted diagnosis of skin cancer: A survey and future recommendations," Comput. Electr. Eng., 104: 108431, 2022.

[5] S. Bakheet, S. Alsubai, A. El-Nagar, A. Alqahtani, "A multi-feature fusion framework for automatic skin cancer diagnostics," Diagnostics, 13(8): 1474, 2023.

[6] S. Fooladi, H. Farsi, S. Mohamadzadeh, "Segmenting the lesion area of brain tumor using convolutional neural networks and fuzzy k-means clustering," Int. J. Eng. Trans. B: Appl., 36(8): 1556-1568, 2023.

[7] N. Ul Huda, R. Amin, S. I. Gillani, M. Hussain, A. Ahmed, H. Aldabbas, "Skin cancer malignancy classification and segmentation using machine learning algorithms," JOM: 1-15, 2023.

[8] Y. Wu, B. Chen, A. Zeng, D. Pan, R. Wang, S. Zhao, "Skin cancer classification with deep learning: a systematic review," Front. Oncol., 12: 893972, 2022.

[9] S. Fooladi, H. Farsi, S. Mohamadzadeh, "Detection and classification of skin cancer using deep learning," J. Birjand Univ. Med. Sci., 26(1): 44-53, 2019.

[10] S. Fooladi, H. Farsi, "Segmentation of cancer cell in histopathologic images of breast cancer and lesion area in skin cancer images using convolutional neural networks," Med. J. Tabriz Univ. Med. Sci. Health Serv., 42(5): 520-528, 2020.

[11] F. Afza, M. Sharif, M. Mittal, M. A. Khan, D. J. Hemanth, "A hierarchical three-step superpixels and deep learning framework for skin lesion classification," Methods, 202: 88-102, 2022.

[12] M. A. Khan, Y. D. Zhang, M. Sharif, T. Akram, "Pixels to classes: intelligent learning framework for multiclass skin lesion localization and classification," Comput. Electr. Eng., 90: 106956, 2021.

[13] M. A. Khan, T. Akram, Y.-D. Zhang, M. Sharif, "Attributes based skin lesion detection and recognition: A mask RCNN and transfer learning-based deep learning framework," Pattern Recognit. Lett., 143: 58-66, 2021.

[14] M. Z. Alom, T. Aspiras, T. M. Taha, V. K. Asari, "Skin cancer segmentation and classification with improved deep convolutional neural network," in Proc. Medical Imaging 2020: Imaging Informatics for Healthcare, Research, and Applications, 11318: 291-301, SPIE, 2020.

[15] G. Nasreen, K. Haneef, M. Tamoor, A. Irshad, "A comparative study of state-of-the-art skin image segmentation techniques with CNN," Multimedia Tools Appl., 82(7): 10921-10942, 2023.

[16] M. Nasir, M. A. Khan, M. Sharif, I. U. Lali, T. Saba, T. Iqbal, "An improved strategy for skin lesion detection and classification using uniform segmentation and feature selection based approach," Microsc. Res. Tech., 81(6): 528-543, 2018.

[17] E. İ. Ünlü, A. Çinar, "Segmentation of benign and malignant lesions on skin images using U-Net," in Proc. 2021 International Conference on Innovation and Intelligence for Informatics, Computing, and Technologies (3ICT): 165-169, 2021.

[18] K. Zafar et al., "Skin lesion segmentation from dermoscopic images using convolutional neural network," Sensors, 20(6): 1601, 2020.

[19] M. Naqvi, S. Q. Gilani, T. Syed, O. Marques, H. C. Kim, "Skin cancer detection using deep learning-A review," Diagnostics, 13(11): 1911, 2023.

[20] M. Asadi-Aghbolaghi, R. Azad, M. Fathy, S. Escalera, "Multi-level context gating of embedded collective knowledge for medical image segmentation," arXiv preprint arXiv:2003.05056, 2020.

[21] M. D. Alahmadi, "Multiscale attention U-Net for skin lesion segmentation," IEEE Access, 10: 59145-59154, 2022.

[22] M. A. Al-Masni, M. A. Al-Antari, M. T. Choi, S. M. Han, T. S. Kim, "Skin lesion segmentation in dermoscopy images via deep full resolution convolutional networks," Comput. Methods Programs Biomed., 162: 221-231, 2018.

[23] C. Zhao, R. Shuai, L. Ma, W. Liu, M. Wu, "Segmentation of skin lesions image based on U-Net++," Multimedia Tools Appl., 81(6): 8691-8717, 2022.

[24] Ş. Öztürk, U. Özkaya, "Skin lesion segmentation with improved convolutional neural network," J. Digital Imaging, 33: 958-970, 2020.

[25] L. Liu, Y. Y. Tsui, M. Mandal, "Skin lesion segmentation using deep learning with auxiliary task," J. Imaging, 7(4): 67, 2021.

[26] H. Wang, J. Yang, "FBUNet: Full convolutional network based on fusion block architecture for biomedical image segmentation," J. Med. Biol. Eng., 41: 185-202, 2021.

[27] S. Mohamadzadeh, S. Pasban, J. Zeraatkar-Moghadam, A. K. Shafiei, "Parkinson's disease detection by using feature selection and sparse representation," J. Med. Biol. Eng., 41(4): 412-421, 2021.

[28] F. Yu, V. Koltun, "Multi-scale context aggregation by dilated convolutions," arXiv preprint arXiv: 1511.07122, 2015.

[29] H. K. Gajera, D. R. Nayak, M. A. Zaveri, "A comprehensive analysis of dermoscopy images for melanoma detection via deep CNN features," Biomed. Signal Process. Control, 79: 104186, 2023.

[30] B. Cassidy, C. Kendrick, A. Brodzicki, J. Jaworek-Korjakowska, M. H. Yap, "Analysis of the ISIC image datasets: Usage, benchmarks and recommendations," Med. Image Anal., 75: 102305, 2022.

[31] K. M. Hosny, D. Elshora, E. R. Mohamed, E. Vrochidou, G. A. Papakostas, "Deep learning and optimization-based methods for skin lesions segmentation: A review," IEEE Access, 11: 85467-85488, 2023.

[32] L. Bi, J. Kim, E. Ahn, D. Feng, "Automatic skin lesion analysis using large-scale dermoscopy images and deep residual networks," arXiv preprint arXiv:1703.04197, 2017.

[33] Z. Yuan, "Automatic skin lesion segmentation with fully convolutional-deconvolutional networks," arXiv preprint arXiv:1703.05165, 2017.

[34] J. Zhu, Z. Liu, W. Gao, Y. Fu, "CotepRes-Net: An efficient U-Net based deep learning method of liver segmentation from computed tomography images," Biomed. Signal Process. Control, 88: 105660, 2024.

[35] M. Niazi, K. Rahbar, "Entropy kernel graph cut feature space enhancement with squeezenet deep neural network for textural image segmentation," Int. J. Image Graphics, 24: 2550064, 2024.

Biographies

Saber Fooladi received a Bachelor's degree in Computer Engineering from Birjand University in Birjand center in 2015 and a Master's degree in Electrical Engineering from Birjand University in Birjand in 2017. Currently, he is a doctoral student in the field of Electrical Engineering and telecommunication Systems. Her research interests include image processing, deep learning, convolutional networks, cloud computing and machine learning.

- Email: saber.fooladi@birjand.ac.ir
- ORCID: 0000-0002-8480-2443
- Web of Science Researcher ID: NA
- Scopus Author ID: NA
- Homepage: NA

Hassan Farsi received the B.Sc. and M.Sc. degrees from Sharif University of Technology, Tehran, Iran, in 1992 and 1995, respectively. Since 2000, he started his Ph.D. in the Centre of Communications Systems Research (CCSR), University of Surrey, Guildford, UK, and received the Ph.D. degree in 2004. He is interested in speech, image and video processing on wireless communications. Now, he works as Associate Professor in Communication Engineering in department of Electrical and Computer Eng., University of Birjand, Birjand, IRAN.

- Email: hfarsi@birjand.ac.ir
- ORCID: 0000-0001-6038-9757
- Web of Science Researcher ID: NA
- Scopus Author ID: 16202385600
- Homepage: https://cv.birjand.ac.ir/hasanfarsi/en

Sajad Mohamadzadeh received the B.Sc. degree in Communication Engineering from Sistan & Baloochestan, University of Zahedan, Iran, in 2010. He received the M.Sc. and Ph.D. degree in Communication Engineering from South of Khorasan, University of Birjand, Birjand, Iran, in 2012 and 2016, respectively. Now, he works as Associte Professor at department of Electrical and Computer Engineering, University of Birjand, Birjand, Iran. His area research interests include Image and Video Processing, Deep Neural Network, Pattern recognition, Digital Signal Processing, Sparse Representation, and Deep Learning.

- Email: s.mohamadzadeh@birjand.ac.ir
- ORCID: 0000-0002-9096-8626
- Web of Science Researcher ID: NA
- Scopus Author ID: 57056477500
- Homepage: https://cv.birjand.ac.ir/mohamadzadeh/en

How to cite this paper:
S. Fooladi, H. Farsi, S. Mohamadzadeh, "Segmentation of skin lesions in dermoscopic images using a combination of wavelet transform and modified U-Net architecture," J. Electr. Comput. Eng. Innovations, 13(1): 151-168, 2025.

DOI: 10.22061/jecei.2024.10807.736

URL: https://jecei.sru.ac.ir/article_2212.html